Available online at www.sciencedirect.com
ScienceDirect
Journal of Sound and Vibration 301 (2007) 649–664
JOURNAL OF SOUND AND VIBRATION
www.elsevier.com/locate/jsvi

Acoustic input impedance of a vibrating cylindrical tube

R. Picó[a,*], F. Gautier[b], J. Redondo[a]

[a]Dept. Física Aplicada, Esc. Politécnica Superior de Gandia, Universidad Politécnica de Valencia, Carretera Nazaret-Oliva s/n, 46700 Valencia, Spain
[b]Laboratoire d'Acoustique de l'Université du Maine, UMR CNRS 6613, Av. O. Messiaen, 72085 Le Mans cedex 9, France

Received 18 March 2004; received in revised form 7 August 2006; accepted 18 October 2006
Available online 19 December 2006

Abstract

An analytical approach to the acoustic input impedance of vibrating cylindrical pipes is considered. The variation in the acoustic impedance introduced by wall vibrations is calculated using the integro-modal method taking into account axisymmetric shell vibration. It is shown that this variation can be interpreted as a small correction in the acoustic input impedance when the walls of the shell do not influence the acoustics in the pipe. Special conditions such as the mechanical resonance condition and spatial coincidence effect lead to maximum values of the correction factor for the input impedance. The results allow us to determine particular shell parameters for which the input impedance is strongly affected by wall vibrations.

1. Introduction

Many applications in mechanical engineering are related to the vibroacoustics of cylindrical shells. In general, these elastic ducts are filled and surrounded with fluid, leading to complex couplings between the structure and the internal and external fluids. This is the case for cylindrical shells, which constitute structure models, such as aircraft fuselages or submarine hulls. Industrial pipes and wind music instruments are other examples of this configuration. When considering such cylindrical tubes as vibroacoustic wave-guides, they can be characterized by their input impedance, which in this case depends on the fluid/structure interaction. The aim of this paper is to develop a model for the input impedance of a vibrating elastic cylindrical shell of finite length simply supported at both ends and filled with fluid. The attention is focused on the interaction between the plane acoustic mode and the symmetric shell modes also known as breathing modes. This model allows us to determine under which conditions shell vibrations can significantly affect the acoustic input impedance. The final application of this study is related to musical acoustics as explained below.

The vibroacoustics of pipes have been extensively studied throughout the literature. Wave propagation inside infinite cylindrical elastic shells containing fluid has been studied in Ref. [1]. Dispersion curves and the energy distribution of free waves of the system are investigated and interpreted. In the case of light fluid, the dispersion curves of the coupled system are found to be close to those of the uncoupled systems. For heavy

*Corresponding author.
E-mail address: rpico@fis.upv.es (R. Picó).

0022-460X/$ - see front matter © 2006 Elsevier Ltd. All rights reserved.
doi:10.1016/j.jsv.2006.10.030

fluids, the fluid-loading term has an important effect on the dispersion curves and leads to complex interpretation of the various branches [2–4]. For applications related to the active control of pipe vibrations, the determination of the response of an infinite elastic fluid-filled shell excited by elementary sources is often required. This is possible using free wave expansions: the case of a harmonic point force excitation (see Ref. [5]), and the case of an interior monopole source (see Ref. [6]) are presented in Ref. [7].

The previously mentioned studies are related to wave propagation into infinite systems. The fact that the propagation modes of the fluid/structure coupled system are not orthogonal means that they are not user-friendly when attempting to describe the behaviour of finite systems. A much more convenient way of doing this is to represent fluid/shell system oscillations using functions associated with the uncoupled systems [8–10]: the displacement field of the shell is expanded over the *in vacuo* structural modes and the inner acoustic field is written as a multimodal expansion using transverse modes of the rigid wave-guide (plane mode and higher order modes). For given excitation conditions, the integro-modal method provides the acoustic and vibratory fields [11–14]. This approach is employed in this paper to describe the interaction between wall vibrations and the air column. The same method has been used in Ref. [15] to compute external radiation impedances, which are useful when describing the external acoustic radiation of the cylinder into light or heavy fluid. In addition, the method has been used in Ref. [16] to determine the internal radiation impedances of a shell of finite length with various acoustic boundary conditions imposed at both ends of the air column. The influence of the mean flow on internal radiation impedances of a finite cylindrical shell with infinite rigid extensions has been studied in Ref. [17].

Wind musical instruments are particular acoustic wave-guides, in which vibroacoustic couplings between the air column and the body of the instrument occur. The walls of the instruments are able to vibrate, resulting in internal and external acoustic radiations. The evaluation of the importance of the role played by these vibrations on the musical sound produced by the instrument is an open question (see Ref. [18] for a bibliography review). In Ref. [19], a vibroacoustic model of a simplified instrument has been proposed in order to quantify the wall vibrations effect that the body has on tone. This simplified instrument consists of a simply supported cylindrical elastic shell filled with and surrounded by fluid. Such a model enables the calculation of the forced response of the system in the frequency domain, taking into account three types of couplings: the shell/internal fluid coupling, the shell/lateral external fluid coupling and the inter-modal coupling induced by acoustic radiation at the end of the tube. Since musical instruments do not work in forced regime, time domain simulations of the self-induced oscillation have been developed for rigid-walled instruments [20]. For these simulations, only the acoustic input impedance characterizes the instrument. The input impedance model presented in this paper is developed in order to be used as input data for time domain simulations of sounds produced by clarinet-like instruments. Since the wall vibrations can either be noted or disregarded, comparisons between these two cases allow us to determine in which case the wall vibration effect is audible. The first results related to these comparisons are available in Ref. [21].

The structure of the paper is as follows: in Section 2, the governing equations of the shell/internal fluid coupled problem are presented. The input impedance is then obtained using projections of the vibratory and acoustic fields on appropriated functional bases: the *in vacuo* shell modes for the structural displacement field and plane wave expansion for the acoustic field. The form of the acoustic impedance at the entrance of the vibrating wave-guide is presented and the effect of wall vibrations is expressed as a correction term of the well-known acoustic impedance of a rigid pipe. In Section 3, attention is focused on the study of the interaction between the acoustic plane wave and the first breathing mode: the structure of the correction term is analysed in detail and the effects of structural resonances and the coincidence effects on the acoustic impedance are discussed using illustrating examples. Finally, a summary of the results is presented.

2. Vibroacoustic model

2.1. Formulation of the problem

We consider a homogeneous, isotropic, thin-walled circular cylindrical shell of length L, mean radius a, and thickness h. The shell material has a Young's modulus E, a Poisson's ratio ν and a density ρ_s. The internal cylindrical cavity is filled with a fluid characterized by its density ρ_0, and its sound speed c. Surfaces S, S_0, S_L

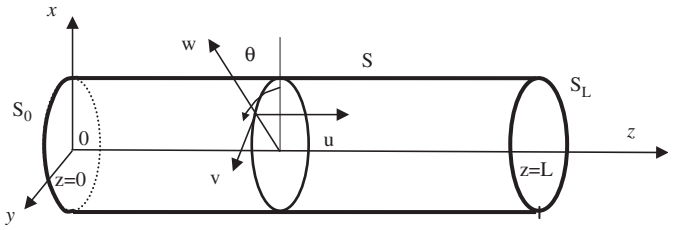

Fig. 1. Notations for the vibrating cylinder.

described in Fig. 1, correspond to the lateral surface of the cylinder ($r = a$), and to the circular surfaces of the cylinder at coordinates $z = 0$ and L, respectively. Let D_i be the fluid domain inside the cylinder, delimited by S, S_0, S_L, and let $\mathbf{n}$ be the unitary normal vector to the cylinder in the outward direction.

The presence of external fluid which surrounds the shell is ignored in this study: it is known that the external fluid/structure coupling leads to added mass and added damping effects for the shell, and also to inter-modal coupling effects [15,18,19]. In the case of light external fluid, these effects can be neglected for the calculation of the shell response and their influence on the acoustic input impedance can be considered as negligible when compared to the influence of inner fluid/shell coupling. As such, we only consider the inner fluid/shell interaction. The excitation of the system consists of a harmonic driving piston which imposes the particle velocity at one end of the tube. The other extremity is supposed to be open. Such a configuration allows us to compute the acoustic input impedance for the vibrating tube.

2.2. Governing equations

In a harmonic regime (the factor $e^{-j\omega t}$ is omitted) two equations govern the problem. The first one is the Helmholtz equation,

$$(\nabla^2 + k^2)p(M) = 0, \quad \text{for } M \in D_i \tag{1}$$

where p is the acoustic pressure inside the cylindrical cavity and $k = \omega/c$ is the acoustic wave number. Dissipative viscothermal effects induced by acoustic boundary layers are considered using the complex wave number k, or in an equivalent way by using a complex sound velocity [12,16]. The Helmholtz equation is associated with appropriate acoustic boundary conditions on surfaces S_0, S, and S_L. On the surface S_0, the acoustic normal velocity V is supposed to be equal to a known value denoted by V_0

$$V(M) = V_0, \quad \text{for } M \in S_0. \tag{2}$$

The acoustic velocity distribution V_0 is supposed to be uniform and can be seen as the excitation source of the system. On the lateral surface S, continuity of the normal velocities of the fluid (denoted by $V_S(M)$) and of the shell (denoted by $\dot{w}(M)$) is expressed as

$$V_S(M) = \dot{w}(M), \quad \text{for } M \in S. \tag{3}$$

On the surface S_L, the tube is supposed to be open. Acoustic radiation into the external fluid through S_L is occurring and can be described using the appropriate impedance condition on surface S_L [22]. Such radiation induces additional inter-modal coupling between the transverse acoustic modes of the waveguide [19]. Since this study is focused upon inner fluid/shell interaction, this phenomenon has not been taken into account. We therefore consider that the acoustic pressure is equal to zero on S_L:

$$p(M) = 0, \quad \text{for } M \in S_L. \tag{4}$$

The second governing equation is the shell motion equation. Generally speaking, the motion of the middle surface of a cylindrical shell can be described by three displacements u, v and w corresponding to longitudinal, circumferential, and radial motions, respectively. When considering only the axisymmetric vibrations, displacements u and w are uncoupled to the torsion motion v. Furthermore, since no mechanical excitation is

imposed in the circumferential direction, the torsional motion v does not play any role and, as such is not considered in the following: the dynamic of the shell can thus be described by a two components vector $\mathbf{X} = [u \;\; w]^t$. In the framework of the Donnell shell theory, the motion equation of the fluid-loaded shell can be written in the following form [23]:

$$-\rho_S h\omega^2 \mathbf{X}(M) - \rho_S h\omega_a^2 \mathscr{L}(\mathbf{X}(M)) = p(M)\mathbf{n}, \quad \text{for } M \in S, \tag{5}$$

where

$$L = \begin{bmatrix} a^2 \dfrac{\partial^2 \cdot}{\partial z^2} & va \dfrac{\partial \cdot}{\partial z} \\ -va \dfrac{\partial \cdot}{\partial z} & -1 - \beta\left(a^2 \dfrac{\partial^2 \cdot}{\partial z^2}\right)^2 \end{bmatrix}, \tag{6}$$

with $\beta = h^2/12a^2$ and $\omega_a = \frac{1}{a}\sqrt{E/(\rho_S(1-v^2))}$. The shell operator $\mathscr{L}$ is the shell Donnell operator written in a simplified form by considering only the axisymmetric vibrations. In Eq. (6), β is a non-dimensional thickness parameter and ω_a denotes the shell ring frequency. Motion Eq. (5) is associated with the mechanical boundary conditions: the shell is supposed to be a simply supported boundary at both ends ($z = 0, L$). This set of particular boundary conditions leads to an analytically tractable solution for the normal *in vacuo* shell modes [23].

This work aims to evaluate the wall vibration effect of a cylinder on its acoustic impedance. To achieve this objective, governing equations (1) and (5), associated to acoustic boundary conditions (2), (3), (4) and simply supported conditions for the shell have to be solved.

2.3. Resolution method

An *in vacuo* modal expansion of the shell displacement field and an integro-modal expression of the inner acoustic pressure field are used in this part in order to formulate two coupled equations from governing form governing equations (1) and (5) of the system.

2.3.1. Modal expansion of the shell displacement field

Since the excitation and the response of the shell are assumed to be axisymmetric, it makes sense to only consider axisymmetric modes for the description of this response. These modes, also called breathing modes, are denoted by $\mathbf{\Phi}_q$ (q being a modal index). Notations and useful results for the computation of their eigenfrequencies and modeshapes are briefly presented in the Appendix A. The shell displacement field is thus expressed as a linear combination of *in vacuo* modes $\mathbf{\Phi}_q$, involving the unknown modal amplitudes A_q

$$\mathbf{X}(M) = \sum_{q=1}^{\infty} A_q \mathbf{\Phi}_q(M), \tag{7}$$

where M is a point located on the middle surface of the shell. Inserting modal expansion (7) into the shell motion equation leads to the following form for the shell motion equation:

$$\rho_S h \sum_q (-\omega^2 + \omega_q^2) A_q \mathbf{\Phi}_q(M) = p(M)\mathbf{n}. \tag{8}$$

By projecting Eq. (8) on a particular mode $\mathbf{\Phi}_q$ and using orthogonal properties of modal basis functions (see relation (A4) in the Appendix A), the motion equation takes the form

$$m_q(-\omega^2 + \omega_q^2) A_q = \langle p(M)\mathbf{n} | \mathbf{\Phi}_q \rangle, \tag{9}$$

where m_q is the modal mass of mode q and where

$$\langle p(M)\mathbf{n} | \mathbf{\Phi}_q \rangle = \int_S p(M)\mathbf{n}\mathbf{\Phi}_q \mathrm{d}S = 2\pi a \int_{z=0}^{z=L} p(z) \sin(q\pi z/L) \mathrm{d}z, \tag{10}$$

is the generalized force acting on the shell. Shell mechanical damping is taken into account by introducing a structural damping term (involving the damping parameter η_q) into Eq. (9) which is finally written as

$$m_q(-\omega^2+\omega_q^2(1-\mathrm{j}\eta_q))A_q=\langle p(M)\mathbf{n}|\mathbf{\Phi}_q\rangle. \tag{11}$$

From expression (11) it can be concluded that if the inner acoustic pressure p is known, the shell modal amplitudes A_q and the shell response $\mathbf{X}(M)$ can be computed: thereby Eq. (11) is the first coupled equation of the problem.

2.3.2. Description of the inner acoustic field using the integro-modal approach

To obtain the inner pressure field, its integral formulation is taken as the starting point [12,13]:

$$p(M)=\int_{S_0,S,S_L}[G(M,M_0)\partial_n P(M)-p(M)\partial_n G(M,M_0)]\mathrm{d}S_0. \tag{12}$$

In a general way, the Green's function of a waveguide $G(M,M_0)$ can be expanded using the propagation modes of the duct. These modes are orthonormal eigenfunctions which are the solutions of the two-dimensional transverse Neumann problem associated with the cross-section of the duct. Since the study is focused only on the acoustic impedance of the plane mode, we limit this expansion to one term, which corresponds to the plane acoustic mode. On each cross section, the acoustic pressure and velocity are thus supposed to be uniform. In this case, the Green's function is written as

$$G(M,M_0)=G(z,z_0)=\frac{\mathrm{j}}{2k\pi a^2}\mathrm{e}^{\mathrm{j}k|z-z_0|}. \tag{13}$$

By replacing expression (13) into the integral representation (12) and after some algebra, the inner acoustic pressure is found to be of the form

$$p(M)=[B^+ + D^+(z)]\mathrm{e}^{\mathrm{j}kz}+[B^- + D^-(z)]\mathrm{e}^{\mathrm{j}k(L-z)}. \tag{14}$$

Thus, the acoustic field can be interpreted as the superposition of two travelling waves in opposite directions with amplitudes depending on z. From Eqs. (12) and (13), it is shown that the amplitudes B^+, B^-, $D^+(z)$, $D^-(z)$ are defined by

$$B^+=\frac{\mathrm{j}}{2k\pi a^2}\int_{S_0}(-\mathrm{j}\rho\omega)V(M)\mathrm{d}S+\frac{1}{2\pi a^2}\int_{S_0}p(M)\mathrm{d}S=\frac{\rho c}{2}\,V_0+\frac{P(0)}{2}, \tag{15}$$

$$B^-=\frac{\mathrm{j}}{2k\pi a^2}\int_{S_L}\mathrm{j}\rho\omega V(M)\mathrm{d}S+\frac{1}{2\pi a^2}\int_{S_L}p(M)\mathrm{d}S=-\frac{\rho c}{2}\,V(L)+\frac{P(L)}{2}, \tag{16}$$

$$D^+(z)=-\frac{\rho_0 c}{a}\int_0^z \mathrm{e}^{-\mathrm{j}kz_0}\dot{w}(z_0)\mathrm{d}z_0, \tag{17}$$

$$D^-(z)=-\frac{\rho_0 c}{a}\,\mathrm{e}^{-\mathrm{j}kL}\int_z^L \mathrm{e}^{\mathrm{j}kz_0}\dot{w}(z_0)\mathrm{d}z_0, \tag{18}$$

where $P(0)$, $P(L)$, V_0, $V(L)$ denote the acoustic pressure and the axial particle velocity at the extremities of the tube ($x=0$ and $x=L$). More useful expressions of the coefficients B^+, B^-, $D^+(z)$, $D^-(z)$ can be computed. Firstly, by applying the acoustic boundary conditions (2) and (4) to the relations (15) and (16), it can be shown that

$$B^+=\frac{1}{1+\mathrm{e}^{2\mathrm{j}kL}}[\rho_0 c V_0+D^-(0)\mathrm{e}^{\mathrm{j}kL}-D^+(L)\mathrm{e}^{2\mathrm{j}kL}], \tag{19}$$

$$B^-=\frac{\mathrm{e}^{\mathrm{j}kL}}{1+\mathrm{e}^{2\mathrm{j}kL}}[-\rho_0 c V_0-D^-(0)\mathrm{e}^{\mathrm{j}kL}-D^+(L)]. \tag{20}$$

Secondly, since coefficients $D^+(z)$, $D^-(z)$ only depend upon the wall vibrations, they can be expressed as functions of the modal amplitudes A_q alone. Indeed, the normal velocity of the shell is obtained by considering

the radial component of the modal expansion (7):

$$\dot{w}(z) = -\mathrm{j}\omega \sum_{q=1}^{\infty} A_q \sin(q\pi z/L). \tag{21}$$

Substituting Eq. (21) in expressions (17) and (18) leads to explicit expressions of the coefficients $D^+(z)$, $D^-(z)$:

$$D^+(z) = \frac{\mathrm{j}\rho_0 c\omega}{a} \sum_q \frac{A_q}{[k^2 - (q\pi/L)^2]} \left[-\frac{q\pi}{L} + \left(\mathrm{j}k \sin \frac{q\pi}{L} z + \frac{q\pi}{L} \cos \frac{q\pi}{L} z \right) \mathrm{e}^{-\mathrm{j}kz} \right], \tag{22}$$

$$D^-(z) = \frac{\mathrm{j}\rho_0 c\omega}{a} \sum_q \frac{A_q}{[k^2 - (q\pi/L)^2]} \left[(-1)^q \frac{q\pi}{L} + \left(\mathrm{j}k \sin \frac{q\pi}{L} z - \frac{q\pi}{L} \cos \frac{q\pi}{L} z \right) \mathrm{e}^{\mathrm{j}k(z-L)} \right]. \tag{23}$$

Relations (19), (20), (22) and (23) show that if the coefficients A_q (or in an equivalent manner the shell radial velocity $\dot{w}$) are known, then the coefficients B^+, B^-, $D^+(z)$, $D^-(z)$ are also known and the inner acoustic pressure can be computed from Eq. (14): Eq. (14) is thus the second coupled equation of the problem.

2.4. Acoustic impedances

The resolution of the coupled equations (11) and (14) is presented in this section, leading to the definition of three kinds of impedance: impedance of the rigid tube, internal radiation impedance and the acoustic impedance of the vibrating tube.

2.4.1. Impedance of the rigid tube and structure of the inner acoustic field

By inspecting relations (19), (20), (22), (23), it can be deduced that whenever the cylinder walls do not vibrate ($\dot{w} = 0$ and $A_q = 0$ for all values of q), then coefficients $D^+(z)$ and $D^-(z)$ are null. This being the case, the acoustic pressure given by Eq. (14) is called blocked pressure, $p_{\mathrm{blocked}}(z)$ and corresponds to the pressure generated in a rigid tube by the input velocity excitation V_0. It can be obtained by considering $V_0 \neq 0$ and by setting $A_q = 0$ in Eqs. (14), (19), (20), (22), (23):

$$p_{\mathrm{blocked}}(z) = -\mathrm{j}\rho_0 c V_0 \frac{\sin k(L-z)}{\cos kL}. \tag{24}$$

When the tube is vibrating, the pressure is written as

$$p(z) = p_{\mathrm{blocked}}(z) + p_{\mathrm{wall}}(z). \tag{25}$$

where $p_{\mathrm{wall}}(z)$ corresponds to the pressure generated by the wall vibrations only. This term is obtained by setting $V_0 = 0$ and by considering $A_q \neq 0$ in Eqs. (14), (19), (20), (22), (23). After some algebra, it is shown that

$$p_{\mathrm{wall}}(z) = -2 \frac{\rho_0 c\omega}{a} \sum_q \frac{A_q}{[k^2 - (q\pi/L)^2]} \left[\frac{q\pi}{L} \frac{\sin k(L-z)}{\cos kz} + \mathrm{j}k \sin \frac{q\pi}{L} z \right]. \tag{26}$$

The input acoustic impedance of the vibrating tube is defined by

$$Z = \frac{p(0)}{V_0} = \frac{p_{\mathrm{blocked}}(0)}{V_0} + \frac{p_{\mathrm{wall}}(0)}{V_0}. \tag{27}$$

The term

$$\frac{p_{\mathrm{blocked}}(0)}{V_0} = -\mathrm{j}\rho_0 c \tan kL = Z_r, \tag{28}$$

corresponds to the input acoustic impedance of the rigid tube. The contribution $p_{\mathrm{wall}}(0)/V_0$ accounts for the wall vibrations. Its calculation requires the computation of the shell response.

2.4.2. Internal radiation impedances and shell response

The shell response is obtained from Eq. (11) in which generalized forces present in the right hand term have to be estimated. The generalized forces associated with the acoustic pressures p_{blocked} and p_{wall} are found to be

$$\langle p_{\text{blocked}}\mathbf{n}|\mathbf{\Phi}_q\rangle_S = 2\text{j}\rho_0 c V_0 \pi a \tan kL \frac{q\pi/L}{k^2-(q\pi/L)^2}, \tag{29}$$

$$\langle p_{\text{wall}}\mathbf{n}|\mathbf{\Phi}_q\rangle_S = \text{j}\omega \sum_{q'} Z_{qq'} A_{q'}, \tag{30}$$

where the impedances $Z_{qq'}$ are called internal radiation impedances. For mutual-impedances ($q \neq q'$), the following is obtained:

$$Z_{qq'} = -\text{j}\rho_0 c S\left(\frac{2(q\pi/L)(q'\pi/L)\tan kL}{aL[k^2-(q\pi/L)^2][k^2-(q'\pi/L)^2]}\right),, \tag{31}$$

where $S = 2\pi aL$ is the surface of the cylinder. For direct or self impedances ($q = q'$), the internal radiation impedance results in

$$Z_{qq} = -\text{j}\rho_0 c S\left(\frac{2(q\pi/L)^2\tan kL}{aL[k^2-(q\pi/L)^2]^2}+\frac{k}{a[k^2-(q\pi/L)^2]}\right). \tag{32}$$

Impedance $Z_{qq'}$ describes the interactions between shell modes $\mathbf{\Phi}_q$ and $\mathbf{\Phi}_{q'}$ via the fluid. The expressions of $Z_{qq'}$ coincide with those obtained in Ref. [16] for the more general case where radial higher order acoustic modes are taken into account for the description of the acoustic field. Writing the shell motion equation in the form

$$m_q\left(-\omega^2-\text{j}\omega\left(\frac{\eta_q}{\omega}+\text{Re}(Z_{qq})\right)+\omega\,\text{Im}(Z_{qq})+\omega_q^2\right)A_q = \langle p_{\text{blocked}}(M)\cdot\mathbf{n}|\mathbf{\Phi}_q\rangle + j\omega\sum_{q'\neq q} A_{q'}Z_{qq'} \tag{33}$$

allows us to give a physical interpretation of these radiation impedances : mutual impedances ($Z_{qq'}$ with $q \neq q'$) describe the inter-modal coupling between different shell modes due to internal acoustic coupling. Direct impedances $Z_{qq} = \text{Re}(Z_{qq}) + \text{j}\,\text{Im}(Z_{qq})$ describe resistive and reactive effects induced by the inner fluid on the structural modes.

For light fluids such as air, the structure is not significantly affected by the fluid loading. Light fluid approximation implies disregarding the coupling terms related to the mutual-impedances $Z_{qq'}$ ($q \neq q'$) in Eq. (33). When employing this approximation, the coefficients of shell modal expansion are obtained from (33) and (29)

$$A_q = \text{j}\rho_0 c V_0 2\pi a \frac{(q\pi/L)\tan kL}{[k^2-(q\pi/L)^2][-m_q\omega^2+m_q\omega_q^2(1-\eta_q)-\text{j}\omega Z_{qq}]}, \tag{34}$$

permitting the shell response to be calculated.

2.4.3. Acoustic impedance of the vibrating tube

Acoustic input impedance of the vibrating tube is finally obtained by substituting Eq. (34) into Eq. (26). This impedance (27) can then be written in the form

$$Z = Z_r(1+C). \tag{35}$$

where coefficient C is given by

$$C = 4\pi\rho_0 c\omega\tan kL\sum_q \frac{(q\pi/L)^2}{[(\omega/c)^2-(q\pi/L)^2]^2[-m_q\omega^2+m_q\omega_q^2(1-\text{j}\eta_q)-\text{j}\omega Z_{qq}]}. \tag{36}$$

It can be seen that the vibrating cylinder impedance Z is the sum of two terms. The first one corresponds to the rigid cylinder impedance Z_r given by Eq. (28), whereas the second is a complementary term equal Z_rC

which depends upon the vibration on the cylinder walls. Coefficient C is called correction coefficient and describes the change in the rigid input impedance induced by the wall vibrations.

3. Wall vibration influence on the input acoustic impedance

3.1. Description of main wall vibration effects

Influence of the inner wall vibration effect on the acoustic input impedance of the tube cylinder can be understood as a correction of the rigid acoustic input impedance, which is studied in this section.

3.1.1. Structure of the impedance correction term

The structure of the impedance correction term can be analyzed by only considering the first breathing mode of the shell. Hence, the correction term is written as

$$C = \frac{4\pi\rho_0 c\omega \tan kL(q\pi/L)^2}{[(\omega/c)^2 - (\pi/L)^2]^2[-m_q\omega^2 + m_q\omega_q^2(1 - j\eta_q) - j\omega Z_{qq}]}, \quad \text{with } q = 1. \tag{37}$$

From Eq. (35) it can be observed that the input acoustic impedance is severely perturbed by the wall vibration if the correction factor C is significant compared to unity. This may be due to several reasons.

The correction factor is inversely proportional to the modal mass m_q which is proportional to the density of the material of the shell. In general terms, this means that the smaller the density of the material is, the bigger the wall vibration effect. The correction factor is also proportional to the factors $[-m_q\omega^2 + m_q\omega_q^2(1 - j\eta_q) - j\omega Z_{qq}]^{-1}$, $[(\omega/c)^2 - (\pi/L)^2]^{-2}$, and $\tan(kL)$. When at least one of these factors takes high values, the correction term also takes high values and the wall vibration effect is important. The conditions $-m_q\omega^2 + m_q\omega_q^2(1 - j\eta_q) - j\omega Z_{qq} \cong 0$ and $(\omega/c)^2 - (\pi/L)^2 \cong 0$ correspond to the structural resonance effects and spatial coincidence effects respectively. The condition $[\tan(kL)]^{-1} = 0$ is the acoustic resonance condition of the associated rigid system. When these effects are produced at similar frequencies, the wall vibration effect becomes important. In order to understand the nature of the effects induced by these three conditions, they will be analyzed separately in the following three paragraphs.

3.1.2. Structural resonance effect

The condition $-m_q\omega^2 + m_q\omega_q^2(1 - j\eta_q) - j\omega Z_{qq} \cong 0$ corresponds to a mechanical resonance condition. For a light fluid the fluid loading is very small and this condition is nearly equivalent to

$$-m_q\omega^2 + m_q\omega_q^2(1 - j\eta_q) \cong 0 \tag{38}$$

For a conservative system ($\eta_q = 0$) this condition is satisfied when the frequency is strictly equal to a shell eigenfrequency. These eigenfrequencies are defined by Eq. (A.7) and are directly dependent on the mechanical and geometrical characteristics of the shell.

3.1.3. Spatial coincidence effect

The correction factor defined by relation (37) inversely depends upon the factor $(\omega/c)^2 - (q\pi/L)^2$. The condition $(\omega/c)^2 - (q\pi/L)^2 = 0$ can only be strictly satisfied if fluid damping is ignored. In this case, the celerity c is real and the condition is satisfied when the acoustic wavenumber $k = \omega/c$ is equal to one of values $q\pi/L = k_q$. This type of condition is a coincidence condition. This wavenumber condition can be read in the frequency domain: each coincidence wavenumber k_q is related to a particular coincidence frequency $f_q = k_q c/2\pi$, which corresponds to an acoustic antiresonance frequency. In other words, each shell mode q produces an alteration in the q-th antiresonance of the input acoustic impedance. This can be explained by the fact that for these antiresonance frequencies, the axial profile of the acoustic pressure along the tube satisfactorily matches one of the shell breathing mode shapes. Indeed, for these frequencies, the acoustic pressure is equal to zero at both ends. The spatial coincidence effect corresponds to the spatial matching condition between the acoustic profile and the structural modes.

If the value of k is close to a coincidence wavenumber, the value for C can be studied using a series expansion: when considering that $k = q\pi/L + \varepsilon$, with $|\varepsilon| \ll 1$, we can write

$$C(k) \propto \frac{\tan(kL)}{[(k)^2 - (q\pi/L)^2]^2} \approx \frac{L^3}{4q^2\pi^2\varepsilon}. \tag{39}$$

Expression (39) shows that the correction factor diverges and tends to an infinite value when $|\varepsilon|$ tends towards zero. Thus, it can be concluded that for a lossless system, the coincidence condition is satisfied exactly at each acoustic antiresonance and induces a divergence of the input acoustic impedance for these values. The effect of the losses consists of a reduction in the influence of this effect upon the global response of the system.

3.1.4. *Effect of the acoustic resonances*

The correction factor is proportional to $\tan(kL)$ (see relation (37)). That means at frequencies for which impedance Z_r is maximum (that is for acoustic resonances frequencies of the rigid tube), the correction factor also takes large values. Thus, the wall vibrations can reinforce the resonance of the acoustic input impedance.

3.2. *Typical numerical applications*

3.2.1. *Characteristics of the system*

With the purpose of illustrating and quantifying the wall vibration effect on the input acoustic impedance, the impedance correction factor C defined by Eq. (37) has been computed numerically in this section for some particular shells. Tables 1 and 2 contain the characteristics of the shell used for the computations: the geometrical parameters of the shell are presented in Table 1 take fixed values for all the cases carried out for all cases conducted henceforth. Having in mind the musical acoustics application described in the introduction, length and radius of the shell are those of a clarinet. The characteristics of the used materials are indicated in Table 2. They have been chosen in order to be illustrative of the different coincidence conditions. It is clear that the chosen material are not realistic if we have in mind the musical application pointed out in the introduction: polymers are not used by instruments' makers to build musical tubes. These materials are only used in our study to illustrate the importance of the various coupling mechanisms. For all computations, the structural damping coefficient has been fixed at $\eta_q = 0.01$ and the viscothermal dissipation in the air column is taken into account by considering that

$$k = \frac{\omega}{c} = \frac{\omega}{c_0} + \alpha(1 - \mathrm{j}), \tag{40}$$

where $\alpha \approx 3.10^{-5}\sqrt{f}/a$ and $c_0 = 343.37\,\mathrm{ms}^{-1}$ at 20 °C (see Ref. [26]).

Table 1
Geometrical parameters of the shell

Radius (a)	7.12 mm
Length (l)	0.5 m
Thickness (h)	0.5 mm

Table 2
Density, Young's modulus and Poisson's ratio of materials used in the numerical applications

Material	Density ρ_S (kg/m^3)	Young's modulus E (10^9 N/m^2)	Poisson's ratio
Steel	7800	210	0.29
Polymer A	1050	1.8	0.33
Aluminum	2710	70	0.33
Wood A	525	13	0.3
Polymer B	1030	0.25	0.3
Polymer C	1030	0.115	0.3

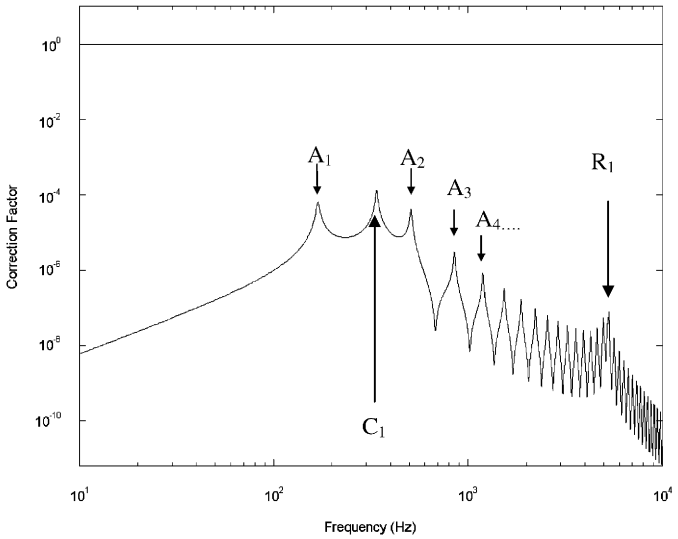

Fig. 2. Magnitude of the correction factor of the acoustic input impedance due to wall vibrations of a cylindrical shell made with steel. Only the first breathing mode (eigenfrequency $f_{R1} = 5188$ Hz) has been considered. Peaks A_i $(i = 1, 2, \ldots)$, C_1 and R_1 indicate the frequencies of the acoustic resonances, of the spatial coincidence condition and of the mechanical resonance respectively.

3.2.2. The case of a steel shell

Fig. 2 shows the magnitude for the correction factor of the input acoustic impedance, induced by the wall vibration effect, when only the interaction between the plane acoustic mode and the first breathing mode is considered. For this numerical application, the shell material is steel. In order to evaluate the importance of wall vibrations, the magnitude of the non-dimensional coefficient C must be compared to unity (horizontal continuous line).

It is found that the wall vibrations have a very small influence on the input impedance since the correction factor C is always lower than 10^{-4}. However, C has some local maxima as previously discussed. Three kinds of peaks, corresponding to the three conditions described in Sections 3.1.2, 3.1.3 and 3.1.4 can be observed. The mechanical resonance frequency of the first breathing mode (referred to as R_1 in Fig. 2) is at $f_{R_1} = 5188$ Hz. The spatial coincidence effect (C_1) is reached for $f_{C_1} = 339$ Hz. As expected (see Section 3.1.4), local maxima for C can also be observed for each acoustic resonance frequency. These are denoted by A_i $(i = 1, \ldots, N)$ in Fig. 2. Except for these local maxima R_1, C_1 and A_i, the correction factor is negligible for all the frequencies of the steel pipe.

3.2.3. The case of a polymer shell

Correction factor C has been computed for a polymer cylinder with the same geometrical features as the previous one. This material is lighter than steel and its Young's modulus is much smaller (see characteristics of polymer A in Table 2). The magnitude of the correction factor for this shell is represented in Fig. 3 as a function of the frequency. It can be seen that the global resonance pattern of the function is similar to that given for steel. However, two main differences can be pointed out: the first being that, in the entire frequency range, the correction factor is greater for polymer than for steel (however, the correction factor C is always lower than 10^{-2}). This can be explained by the fact that the correction factor is inversely proportional to the wall density of the shell. The second difference is that the mechanical resonance R_1 is much smaller for the polymer $f_{R_1} \approx 1309$ Hz than for steel. Thus, the local maximum of $|C|$ due to R_1 is observed at a lower frequency than is the case for the steel shell.

In Fig. 4a, the vibrating acoustic input impedances of four cylinders made of different materials have been plotted: steel, aluminium, wood A (Epicea) and polymer A. The impedance of a rigid tube has also been plotted for comparison. The Young's modulus and density of the used materials are shown in Table 2. No differences can be seen except for a small shift of frequency in the case of the polymer shell: the representation is focused on the first antiresonance of the shells in Fig. 4b, which corresponds to the coincidence condition of

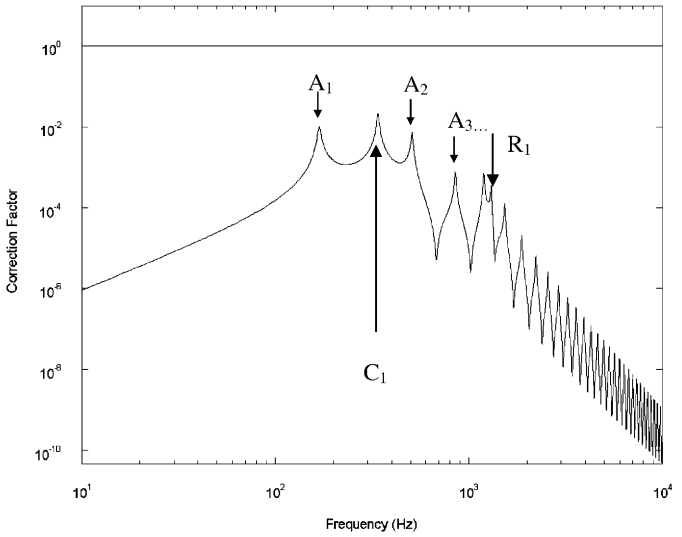

Fig. 3. Magnitude of the correction factor of the acoustic input impedance due to the wall vibrations of a cylindrical shell made by polymer A. Only the first breathing mode (eigenfrequency $f_{R1} = 1309\,\text{Hz}$) has been considered.

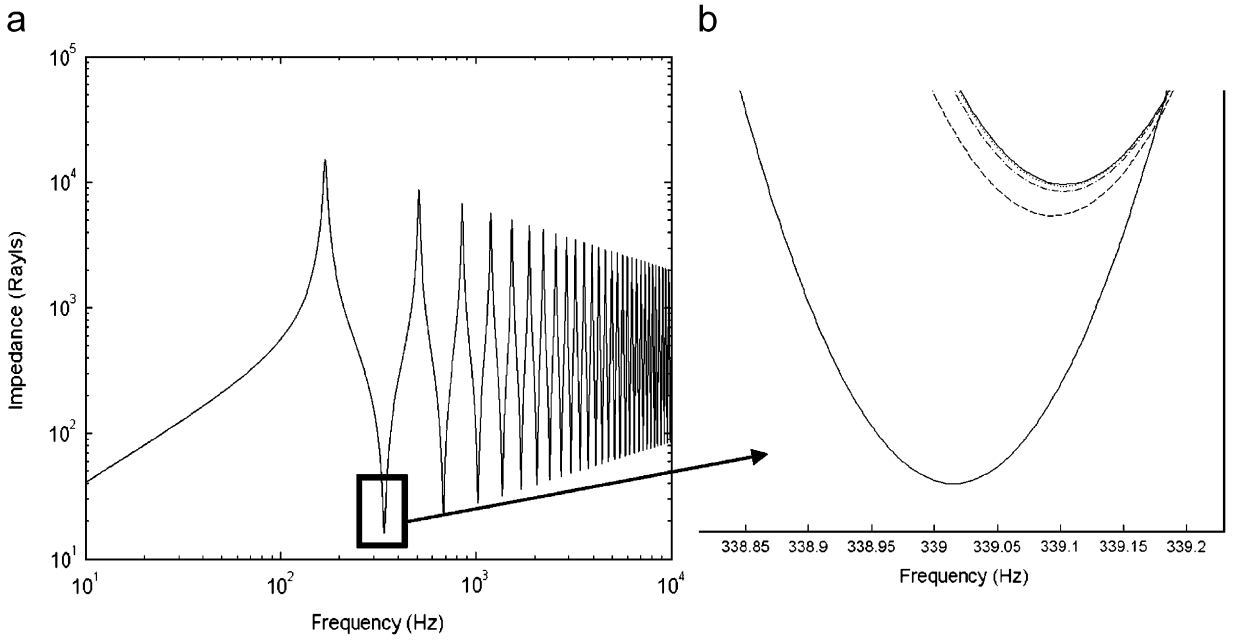

Fig. 4. (a) Acoustic input impedance of ——— a rigid tube compared with four vibrating shells made of ····· steel, —·— aluminium, - - - - wood A and ▬▬ polymer A. For each case, only the breathing mode has been considered. (b) Zoom at the first antiresonance of the acoustic input impedance.

the first breathing mode. It can be noted that the lower the density of the shell material, the more important the shift in the antiresonance frequency. However, this effect remains very small.

3.3. Special material parameters leading to strong vibroacoustic coupling

For some specific frequency conditions, shell modes interact strongly with acoustic modes, leading to important changes in the acoustic response of the tube. These conditions are satisfied for special material parameters, given for each case. In this part, several special phenomena linked to shell/fluid coupling are studied.

3.3.1. The case of a mechanical resonance close to an acoustical resonance

If the eigenfrequency of the first breathing shell mode is close to an acoustic resonance, an important alteration in the input acoustic impedance next to the acoustic resonance peak can be observed. In this case, the correction factor actually takes large values when the frequency is in the vicinity of the first resonance frequency. This is due to the fact that in the expression of C (see Eq. (37)), both terms $\tan(kL)$ and $(-m_q\omega^2 + m_q\omega_q^2(1-\mathrm{j}\eta_q) - \mathrm{j}\omega Z_{qq})^{-1}$ take high values. A numerical application has been carried out in the case of a polymer shell. Its characteristics are given in Table 2 (polymer B). The choice of these parameters is achieved in such a way that the frequency of the first breathing mode ($f_{R_1} = 492\,\mathrm{Hz}$) is close to the second acoustic resonance ($f_2 = 510\,\mathrm{Hz}$). In these conditions, the acoustic impedance is strongly modified by the wall vibrations as shown in Fig. 5a and b.

3.3.2. Mechanical resonance and spatial coincidence effects simultaneously satisfied

When the mechanical resonance and the coincidence condition are produced at close frequencies, the wall vibration effect becomes drastically important. Indeed, in the expression of C (see Eq. (38)), both terms $((\omega/c)^2 - (q\pi/L)^2)^{-2}$ and $(-m_q\omega^2 + m_q\omega_q^2(1-\mathrm{j}\eta_q) - \mathrm{j}\omega Z_{qq})^{-1}$ take large values. In order to illustrate this configuration, the Young's modulus and the density of the material of polymer C (see Table 2) are determined in a way that the shell resonance ($f_{R_1} = 334\,\mathrm{Hz}$) is produced nearly at the frequency of the first acoustic antiresonance ($f_{C_1} = 339\,\mathrm{Hz}$). The correction factor for this frequency presents a significant peak which is much higher than unity. As it can be seen in Fig. 6, the acoustic input impedance of the vibrating cylindrical shell drastically changes. The wall vibration effect becomes so important that the acoustic behaviour of the shell is no longer comparable to the equivalent rigid shell.

3.4. Multimodal model analysis

In Section 3.3, the shell modal expansion has been restricted to the first shell-breathing mode, allowing the identification and an understanding of the main coupling effects. In this section, the effect of several breathing modes on the tube input acoustic impedance is considered. The cases of 2 and 10 modes are presented and allow us to generalize with regards to the conclusions of the previous section.

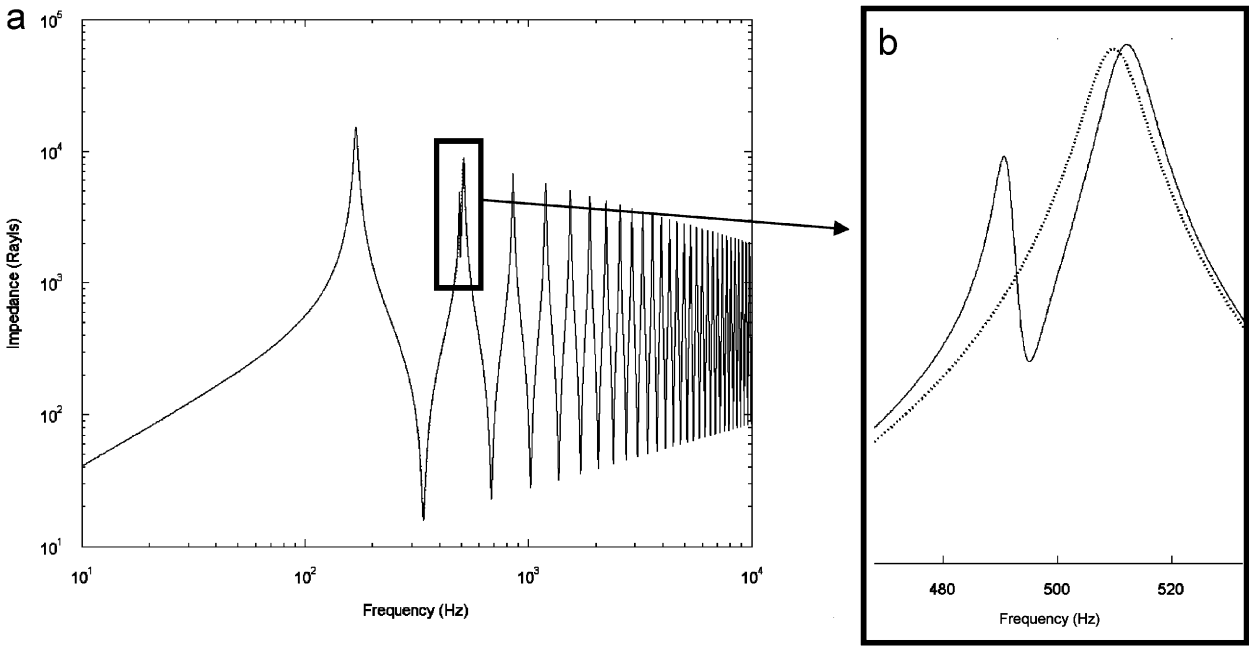

Fig. 5. (a) Acoustic input impedance of a ⋯⋯ rigid cylinder and a wall vibrating cylinder made of ——— polymer B. Only the first breathing mode (eigenfrequency $f_{R1} = 492\,\mathrm{Hz}$) has been considered. (b) Zoom at the second acoustic resonance.

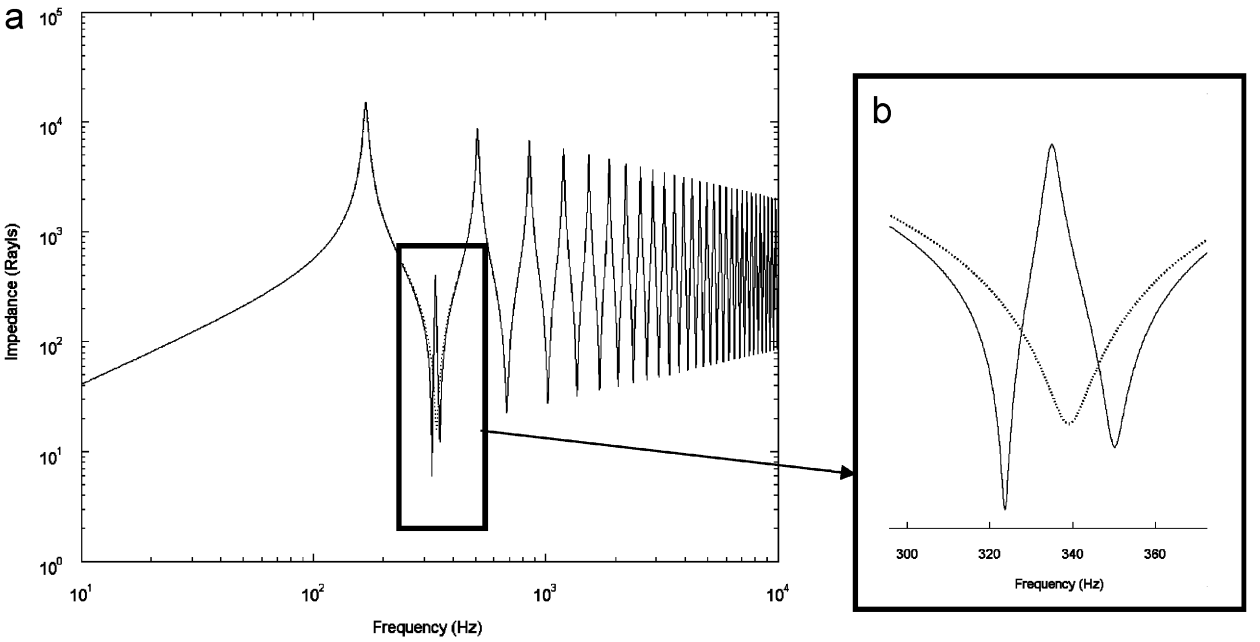

Fig. 6. (a) Acoustic input impedance of a ····· rigid cylinder and a wall vibrating cylinder made with ——— polymer C. Only the first breathing mode ($f_{R1} = 334$ Hz) has been considered. (b) Zoom at the first acoustic antiresonance.

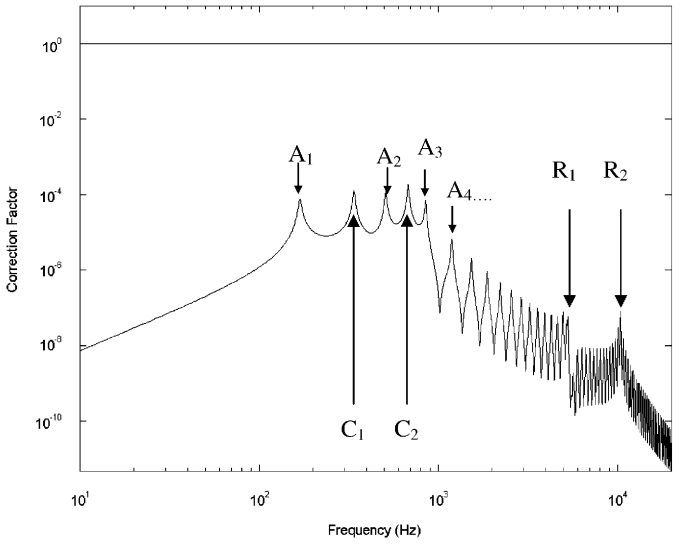

Fig. 7. Magnitude of the correction factor of the acoustic input impedance induced by the wall vibration of a steel shell. The first ($q = 1$, $f_{R1} = 5188$ Hz) and the second ($q = 2$, $f_{R2} = 10374$ Hz) breathing modes are considered.

The magnitude of the correction factor is shown in Fig. 7 for two shell modes ($q = 1$ and 2) for a shell made of steel. The consequence of considering two shell modes is that two coincidences and two resonances exist and lead to local maxima in the correction factor. Both spatial coincidence conditions are satisfied at frequencies $f_{C_1} = 339$ and $f_{C_2} = 678$ Hz. The two resonance conditions are satisfied at frequencies $f_{R_1} = 5188$ and $f_{R_2} = 10374$ Hz.

The wall vibration effect of a great number of mechanical modes is now considered. The truncation of the structural bases is fixed on 10 mechanical modes. Fig. 8 shows the magnitude of the correction factor for the

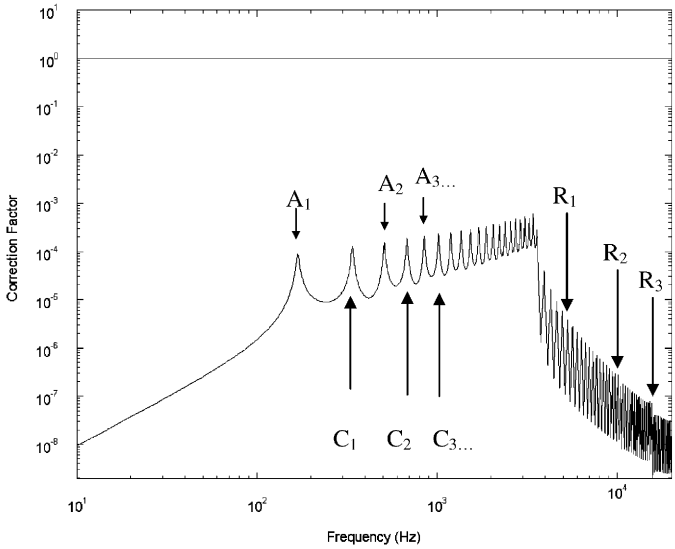

Fig. 8. Magnitude of the correction factor of the acoustic input impedance induced by the wall vibration of a steel shell. The structural modal basis has been truncated at 10 modes.

input acoustic impedance, whose physical interpretation is the natural extension of the previous cases: maxima for the correction factor are found when spatial coincidence conditions, mechanical resonance conditions or acoustic resonance conditions are satisfied.

4. Conclusions

A vibroacoustic model of a simply supported thin cylindrical shell has been developed in order to evaluate the inner fluid/shell coupling and quantify the wall vibration effect on its acoustic behaviour. The input acoustic impedance of the tube vibrating has been obtained analytically and can be understood as a very small variation of the plane mode impedance of an equivalent rigid cylinder. The plane acoustic mode, which is dominant below the first cut-off frequency interacts with the shell modes which have the same symmetry, and as such, this is only coupled to the shell breathing modes. It is found that in general the vibroacoustic coupling is negligible, which leads to a very small correction of the input impedance. However, for some special materials, the wall vibration effect becomes very important. Three phenomena underlie this singular behaviour: a mechanical resonance; a spatial coincidence effect; and, an acoustic resonance. If two of these phenomena occur simultaneously, the perturbation effect becomes significant and the acoustic resonances and antiresonances of the tube can be significantly altered.

The application, which has motivated this study concerns the quantitative evaluation of the influence of the wall vibrations of a wind instrument on the emitted sound. Since the coupling between shell and internal fluid is very weak, one can expect that wall vibration does not disturb the acoustical behaviour of the instrument in a significant way. For classical materials used by instruments' maker (wood or metal) and for a geometry close to the one of the clarinet, the fact that this perturbation is very small is mostly due to the fact that breathing modes of the tube have very high eigenfrequencies. However, it is known that the first modes of a shell are generally not the breathing modes but involves asymmetric motions of the cross sections. This is the case of ovalling modes for example. In a theory in which no faults in symmetry are considered, these asymmetric modes are not coupled to the acoustic plane modes which is dominant at low frequency and which govern the acoustic behaviour of the instrument. When small faults in symmetry, which always exist in practical cases are considered, additional coupling between ovalling modes and acoustic plane modes have to be considered.

Acknowledgements

The authors would like to thank Joel Gilbert his comments and also for the helpful discussions.

Appendix A. Structural modal basis

The aim of this appendix is to briefly review the main results, that permit the computation of the *in vacuo* shell breathing modes $\mathbf{\Phi}_q$. These modes are axisymmetric and involve only coupled motions in the axial and radial directions. Their modeshape can be written as [23,24]

$$\mathbf{\Phi}_q = \begin{bmatrix} U_q \cos(q\pi z/L) \\ W_q \sin(q\pi z/L) \end{bmatrix}, \tag{A.1}$$

where the ratio between the modal amplitudes U_q and W_q is given by

$$\frac{U_q}{W_q} = \frac{\nu(q\pi a/L)}{(q\pi a/L)^2 - (\omega_q/\omega_a)^2}. \tag{A.2}$$

In this paper, the normalization convention for modes $\mathbf{\Phi}_q$ is given by $W_q = 1$. The mode $\mathbf{\Phi}_q$, associated to the eigenfrequency ω_q is the solution of the conservative homogeneous problem

$$\rho_S h(\omega_a^2 \mathscr{L} + \omega_q^2)\mathbf{\Phi}_q = 0, \tag{A.3}$$

and satisfies a mass weighted orthogonality relationship [25],

$$\langle \mathbf{\Phi}_q | \mathbf{\Phi}_{q'} \rangle = \int_S \mathbf{\Phi}_q \mathbf{\Phi}_{q'} \rho_S h \, \mathrm{d}S = m_q \delta_{qq'}, \tag{A.4}$$

where $\delta_{qq'}$ is the Kronecker notation, and where the generalized mass or modal mass m_q is given by

$$m_q = \rho_S h \pi a l (U_q^2 + W_q^2). \tag{A.5}$$

The eigenfrequency ω_q is the solution of the equation

$$|\omega_a^2 \mathscr{L} + \omega_q^2| = 0, \tag{A.6}$$

obtained by inserting Eq. (A.1) into the homogeneous motion Eq. (A.3). For the Donnell theory and by only considering the breathing motions, this equation can be written as

$$(\omega_q/\omega_a)^4 - K_2(\omega_q/\omega_a)^2 + K_0 = 0, \tag{A.7}$$

where $K_0 = (1-\nu^2)(q\pi a/L)^4 + \beta(q\pi a/L)^6$ and $K_2 = 1 + (q\pi a/L)^2 + \beta(q\pi a/L)^4$. For the two solutions ω_q of Eq. (A.6) the amplitude U_q can be calculated from Eq. (A.1). For thin and slender shells ($a/L < 1$), only the smaller solution has to be taken into account as the other solution is in the ultrasound-range frequency.

References

[1] C.R. Fuller, F.J. Fahy, Characteristics of wave propagation and energy distributions in cylindrical elastic shells filled with fluid, *Journal of Sound and Vibration* 81 (4) (1982) 501–518.
[2] K. Trdak Intensités vibratoire et acoustique dans les tuyaux, PhD Thesis, Université de Technologie de Compiègne, France, 1995 (in French).
[3] B.J. Brevart, C.R. Fuller, Active control of coupled wave propagation in fluid-filled elastic cylindrical shells, *Journal of the Acoustical Society of America* 94 (3) (1993) 1467–1475.
[4] L. Feng, Acoustic properties of fluid-filled elastic pipes, *Journal of Sound and Vibration* 176 (3) (1994) 399–413.
[5] C.R. Fuller, The input mobility of an infinite circular cylindrical elastic shell filled with fluid, *Journal of Sound and Vibration* 87 (3) (1983) 409–427.
[6] C.R. Fuller, Monopole excitation of vibrations in an infinite cylindrical elastic shell filled with fluid, *Journal of Sound and vibration* 96 (1) (1984) 101–110.
[7] C. Fuller, S. Elliott, P.A. Nelson, *Active Control of Vibration*, Academic Press, New York, 1996.

[8] M.C. Junger, D. Feit, Sound Structures and their Interaction, published by the Acoustical Society of America through the American Institute of Physics, 1993.
[9] J.L. Guyader, B. Laulagnet, Structural Acoustic radiation prediction: expanding the vibratory response on a functional basis, *Applied Acoustics* 43 (1994) 247–269.
[10] B. Laulagnet, Modal method in sound radiation problems: academic and more complicated cases, *Euro-noise 95 Proceedings* (1995) 363–373.
[11] C. Lesueur, Rayonnement acoustique des structures, Editions Eyrolles, 1988 (in French).
[12] M. Bruneau, Manuel d'Acoustique fondamentale, Editions Hermes, Paris, 1998 (in French).
[13] P.M. Morse, K.U. Ingard, *Theoretical Acoustics*, Princeton University Press, 1986.
[14] S.E. Hassan, P.R. Stepanishen, Response of force excited elastic solids with internal fluid loading, *Journal of the Acoustical Society of America* 116 (2) (2004) 891–899.
[15] B. Laulagnet, J.L. Guyader, Modal analysis of a shell's acoustic radiation in light and heavy fluids, *Journal of Sound and Vibration* 131 (3) (1989) 397–415.
[16] F. Gautier, N. Tahani, Vibroacoustics of cylindrical pipes: internal radiation modal coupling, *Journal of Sound and Vibration* 215 (5) (1998) 1165–1179.
[17] N. Ouelaa, B. Laulagnet, J.L. Guyader, Etude vibro-acoustique d'une coque cylindrique finie remplie de fluide en mouvement uniforme, *Acta Acustica* 2 (1994) 275–289 (in French).
[18] F. Gautier, Contribution à l'étude du comportement vibroacoustique des instruments de musique à vent, PhD Thesis, Université du Maine, Le Mans, France, 1997 (in French).
[19] F. Gautier, N. Tahani, Vibroacoustic behavior of a simplified musical wind instrument, *Journal of Sound and Vibration* 213 (1998) 107–125.
[20] B. Gazengel, J. Gilbert, N. Amir, Time domain simulation of single reed wind instrument. From the measured input impedance to the synthesis signal. Where are the tramps ?, *Acustica* 3 (1995) 445–472.
[21] R. Picó Vila, J. Gilbert, F. Gautier, Study of the input acoustic impedance of a vibrating cylindrical shell: consequences on clarinet-like instrument, Proceedings of the Seventh CFA/DAGA, Strasbourg, France, 22–25 March 2004.
[22] W.E. Zorumsky, Generalized radiation impedance and reflection coefficients of circular and annular ducts, *Journal of Acoustical Society of America* 154 (6) (1973) 1667–1673.
[23] A.W. Leissa, *Vibrations of Shells*, NASA, Washington, DC, 1973.
[24] W. Soedel, *Vibrations of shells and plates, Hardcover*, second ed., 1993.
[25] M. Géradin, D. Rixen, Théorie des vibrations. Application à la dynamique des structures. Ed. Masson, 1992 (in French).
[26] R. Causse, J. Kergomard, X. Lurton, Input impedance of brass musical instruments—Comparison between experiment and numerical models, *Journal of the Acoustical Society of America* 75 (1984) 241–254.